



Available online at <http://scik.org>

Commun. Math. Biol. Neurosci. 2025, 2025:45

<https://doi.org/10.28919/cmbn/9140>

ISSN: 2052-2541

MODELING NIPAH VIRUS DYNAMICS AND DESIGNING OPTIMAL CONTROL STRATEGIES

ZARHOUTI MOHAMED KHALIL^{1,*}, MOHAMMED RIMI², JAMAL MOULINE²

¹Interdisciplinary Research Laboratory: Sciences, Education and Training (IRLSET), Higher School of Education and Training, Berrechid, Hassan 1st University, Settat, Morocco

²Laboratory of Analysis Modeling and Simulation, Department of Mathematics and Computer Science, Faculty of Sciences Ben M'sik, Hassan II University of Casablanca, Morocco

Copyright © 2025 the author(s). This is an open access article distributed under the Creative Commons Attribution License, which permits unrestricted use, distribution, and reproduction in any medium, provided the original work is properly cited.

Abstract. This study introduces a mathematical model designed to shed light on how Nipah virus (NiV) spreads. The model emphasizes the application of control strategies to contain the virus, considering two primary transmission pathways: direct contact and transmission through animal hosts, especially bats and pigs. The goal is to deepen our understanding of how the virus spreads and to propose strategies that aim to reduce the number of infections and increase recoveries during the observation period, all while keeping the costs of these strategies low. The mathematical framework provided enables the combination of different control strategies to effectively manage the transmission dynamics of Nipah virus. By utilizing Pontryagin's maximum principle, we identify effective measures to curb the disease's spread. Theoretical findings are then validated through numerical simulations performed using MATLAB.

Keywords: nipah virus; optimal control; spread of nipah.

2020 AMS Subject Classification: 92D30.

*Corresponding author

E-mail address: m.mohamed.baroudi@gmail.com

Received January 20, 2025

1. INTRODUCTION

Nipah virus (NiV) is a zoonotic virus, meaning that it is transmitted from animals to humans. The virus is primarily transmitted through contact with infected pigs and bats, particularly the *Pteropus* species, which are known as the natural reservoir for the virus. Nipah virus is classified under the genus *Henipavirus* and is known for causing severe and deadly outbreaks in humans [1, 2, 3]. Since its first discovery in 1998 during an outbreak in Peninsular Malaysia, where individuals involved in pig farming were among the first infected, Nipah virus has become a significant public health threat. The fatality rate associated with NiV infections is extremely high, ranging between 40% and 75% depending on the outbreak and the availability of supportive care. This high mortality rate, combined with the lack of licensed vaccines or antiviral treatments, has led the World Health Organization (WHO) to classify Nipah virus as one of the top ten priority diseases for research and development according to the WHO Research and Development Blueprint [4, 5, 6, 7].

Our work seeks to model the Nipah virus using differential equations to address concrete problems such as the spread of Nipah virus within a biological context. This approach employs a rigorous mathematical framework and is based on two types of mathematization, as proposed by Barnes (see figure) [8]:

- **Horizontal mathematization**, where mathematical tools are employed to structure and solve a real-world situation (here, the dynamics of Nipah virus) into a mathematical model.
- **Vertical mathematization**, which occurs at a purely mathematical level, focusing on mathematical language and treatment.

The figure below illustrates the two aforementioned phases. Horizontal mathematization involves describing the real-world situation and the inherent information within reality, schematized as “describing.” On the other hand, vertical mathematization focuses on translating these aspects into mathematical language and mathematical treatment, indicated respectively by “Mathematical language” and “Algorithm.”

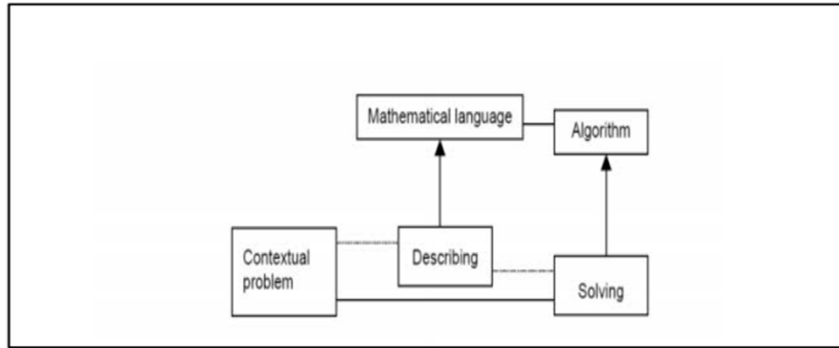


FIGURE 1. Horizontal and Vertical Mathematization Phases in Modeling Nipah Virus Dynamics

The critical importance of this research is highlighted by the ongoing and widespread nature of Nipah virus outbreaks. Since its initial discovery, the virus has not been confined to Malaysia; instead, Nipah has caused outbreaks in several other countries, including Bangladesh [9, 10, 11], India, and Singapore. In Bangladesh and India, Nipah virus outbreaks occur almost annually, leading to numerous deaths and raising significant concerns about the virus’s potential to cause a global pandemic. The figure below (Figure 2) illustrates the evolution of reported cases and fatalities from Nipah virus outbreaks over the years, based on WHO data. This chart emphasizes the persistence of the virus and its potential for resurgence, particularly in areas where bats and pigs coexist with human populations.

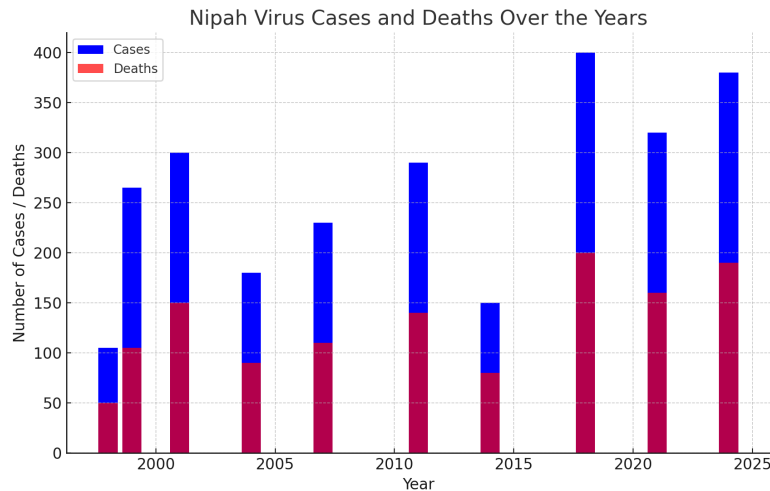


FIGURE 2. Evolution of Nipah Virus Cases and Fatalities Over the Years (Source: WHO)

Extensive research has been conducted to understand Nipah virus, utilizing various mathematical models and studies. For example, researchers have proposed a model that includes the role of deceased individuals who succumbed to Nipah fever, highlighting the importance of considering the deceased in transmission dynamics. Others have developed a model focusing on Nipah virus transmission through human-pig interactions, which is crucial for understanding the virus's spread in rural farming communities. Additionally, a model [12] based on the SIRD framework has been introduced, considering the transmission of infection from infected corpses to living humans, underscoring the need to manage infected corpses properly to prevent further spread [13, 14, 15, 16, 17, 18, 19, 20, 21].

Given the significant threat posed by Nipah virus, it is essential to develop and implement effective strategies to control its spread. The second part of this research focuses on exploring the necessity and effectiveness of various control measures that can be used to reduce the transmission of Nipah virus among human populations. These strategies are necessary not only to address the immediate risks posed by Nipah but also to prevent future outbreaks, which could have devastating effects on public health and global security.

Despite these comprehensive efforts, most models [22, 23, 24] have not adequately addressed the direct transmission of Nipah virus from bats and pigs to humans. Furthermore, these models often lack a focus on the dynamics and optimal control strategies for virus transmission. To address these gaps, we propose a more detailed and realistic mathematical model to examine Nipah virus transmission between pigs and humans, as well as its transmission from person to person.

One of the most critical control measures, denoted as v , involves minimizing contact with infected individuals, pigs, and bats. This strategy is of utmost importance as it directly addresses the primary modes of Nipah virus transmission. Pigs have been identified as a significant amplifying host for the virus, particularly during the initial outbreak in Malaysia, where the virus rapidly spread among pig populations and then to humans. To reduce the risk of transmission, it is essential to implement strict biosecurity measures in pig farming practices, such as isolating sick animals, enforcing quarantine protocols, and controlling the movement of livestock. Additionally, efforts to reduce bat-to-human transmission must focus on preventing bats from

contaminating food sources, such as date palm sap, which is commonly consumed in many endemic regions. Communities in these areas should be educated on the importance of boiling date palm sap before consumption and avoiding fruits that show signs of bat bites.

The second control measure, denoted as w , focuses on the importance of public awareness campaigns and potential vaccination strategies. Although no vaccine currently exists for Nipah, raising public awareness about the risks associated with the virus and educating communities on preventive measures can significantly reduce the likelihood of transmission. Public health campaigns should focus on educating individuals about the symptoms of Nipah, the importance of seeking early medical attention, and the measures they can take to protect themselves and their families. Furthermore, research into vaccine development for Nipah is ongoing, and it is crucial to prepare for the potential deployment of a vaccine in the future. Vaccination, when available, will be a critical tool in controlling Nipah outbreaks and preventing the spread of the virus to new regions.

This research is motivated by the need to fill gaps in our understanding of Nipah virus transmission dynamics and to develop effective public health interventions that can mitigate the impact of the virus. By integrating the control strategies u and v into a comprehensive mathematical model, this study aims to provide a robust framework for predicting and controlling Nipah outbreaks. This model will not only help public health officials respond more effectively to current and future outbreaks but will also contribute to global efforts to prevent a potential pandemic. The ultimate goal of this research is to reduce the burden of Nipah virus on affected populations, protect vulnerable communities, and enhance global health security. In conclusion, as the threat of Nipah virus continues to emerge in various regions of the world, particularly in South and Southeast Asia, it is crucial that we invest in research that advances our understanding of the virus and its transmission. The development and implementation of effective control strategies, supported by rigorous scientific research, will be key to mitigating the impact of this deadly virus and preventing future outbreaks. Through this research, we hope to contribute to global efforts to combat Nipah virus and safeguard public health.

In the first section of the document, we introduce some basic characteristics and definitions of the disease. Following this, the second section provides a mathematical model to understand

the dynamics of the virus transmission. The third section reviews the mathematical models used to delve deeper into these transmission dynamics. The fourth section is dedicated to discussing control strategies and preventive measures aimed at limiting the transmission of the Nipah virus. Finally, the fifth section concludes the discussion by emphasizing the global importance of ongoing research and development related to the Nipah virus and its significant impact on global public health.

2. MODEL FORMULATION

To study the evolution of Nipah virus transmission dynamics, we will divide the pigs population into two epidemiological categories: susceptible animals S_a and infected animals I_a . The total number of pigs is denoted by N_a , which satisfies the equation $N_a = S_a + I_a$. Similarly, the total number of people N_h is divided into the following categories: susceptible S , exposed E , infected I , vaccinated V and recovered R , which satisfies the equation $N_h = S + E + I + V + R$. Figure (3) provides a visual illustration of the model being proposed.

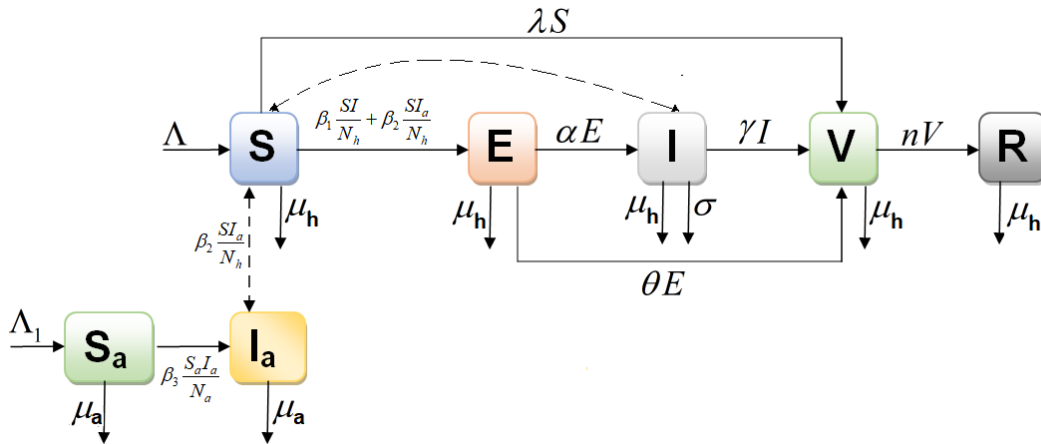


FIGURE 3. Model of human and animal population compartments.

The different compartments of our model are listed in table (1) below, detailing their respective descriptions. This table provides a comprehensive overview of each compartment's role within the model.

Compartment	Description
S	The number of individuals susceptible to the virus.
E	The number of infected individuals without symptoms.
I	The number of symptomatic infected individuals.
V	The number of individuals who are hospitalized.
R	The number of recovered individuals.
S_a	The number of pigs susceptible to the virus.
I_a	The number of infected pigs.

TABLE 1. A description of the various compartments within our model.

Therefore, we present a mathematical model that is governed by the following system of differential equations.

$$(1) \quad \left\{ \begin{array}{l} \frac{dS(t)}{dt} = \Lambda - \beta_1 \frac{S(t)I(t)}{N_h} - \beta_2 \frac{S(t)I_a(t)}{N_h} - (\lambda + \mu_h)S(t), \\ \frac{dE(t)}{dt} = \beta_1 \frac{S(t)I(t)}{N_h} + \beta_2 \frac{S(t)I_a(t)}{N_h} - (\alpha + \theta + \mu_h)E(t), \\ \frac{dI(t)}{dt} = \alpha E(t) - (\gamma + \mu_h + \sigma)I(t), \\ \frac{dV(t)}{dt} = \gamma I(t) + \lambda S(t) + \theta E(t) - (n + \mu_h)V(t), \\ \frac{dR(t)}{dt} = nV(t) - \mu_h R(t), \\ \frac{dS_a(t)}{dt} = \Lambda_1 - \beta_3 \frac{S_a(t)I_a(t)}{N_a} - \mu_a S_a(t), \\ \frac{dI_a(t)}{dt} = \beta_3 \frac{S_a(t)I_a(t)}{N_a} - \mu_a I_a(t). \end{array} \right.$$

where $S(0), E(0), I(0), V(0), R(0), S_a(0)$ and $I_a(0) \in \mathbb{R}_+^*$ represent the specified initial state.

2.1. Model basic properties.

2.1.1. Positivity of solutions.

Theorem 1.

If $S(0) \geq 0, E(0) \geq 0, I(0) \geq 0, V(0) \geq 0, R(0) \geq 0, S_a(0) \geq 0$, and $I_a(0) \geq 0$ are specified, then the solutions of system (1) remain non-negative for all $t \geq 0$.

Proof.

Upon examining the initial equation in system (1), it becomes clear that.

$$(2) \quad \frac{dS(t)}{dt} = \Lambda + \left(-\beta_1 \frac{I(t)}{N_h} - \beta_2 \frac{I_a(t)}{N_h} - \lambda - \mu_h \right) S(t) \geq - \left(\beta_1 \frac{I(t)}{N_h} + \beta_2 \frac{I_a(t)}{N_h} + \lambda + \mu_h \right) S(t),$$

$$(3) \quad \frac{dS(t)}{dt} + \left(\beta_1 \frac{I(t)}{N_h} + \beta_2 \frac{I_a(t)}{N_h} + \lambda + \mu_h \right) S(t) \geq 0.$$

Where

$$L(t) = \beta_1 \frac{I(t)}{N_h} + \beta_2 \frac{I_a(t)}{N_h} + \lambda + \mu_h,$$

$$(4) \quad \frac{dS(t)}{dt} + L(t)S(t) \geq 0.$$

By multiplying both sides of the inequality by $\exp\left(\int_0^t L(s)ds\right)$, we obtain

$$(5) \quad \exp\left(\int_0^t L(s)ds\right) \frac{dS(t)}{dt} + L(t) \exp\left(\int_0^t L(s)ds\right) S(t) \geq 0,$$

$$(6) \quad \frac{d}{dt} \left(S(t) \exp\left(\int_0^t L(s)ds\right) \right) \geq 0.$$

Calculating the integral of this inequality from 0 to t results in:

$$(7) \quad \int_0^t \left(\frac{d}{ds} \left(S(s) \exp\left(\int_0^s L(s)ds\right) \right) \right) ds \geq 0,$$

then

$$S(t) \geq S(0) \exp\left(\int_0^t L(s)ds\right),$$

$$(8) \quad S(t) \geq 0.$$

The second equation of system (1) implies that:

$$(9) \quad \begin{aligned} \frac{dE(t)}{dt} &= \beta_1 \frac{S(t)I(t)}{N_h} + \beta_2 \frac{S(t)I_a(t)}{N_h} - (\alpha + \theta + \mu_h)E(t) \\ &\geq -(\alpha + \theta + \mu_h)E(t). \end{aligned}$$

Then

$$(10) \quad \frac{dE(t)}{dt} + (\alpha + \theta + \mu_h)E(t) \geq 0.$$

The last inequality is multiplied by $\exp((\alpha + \theta + \mu_h)t)$ on both sides, we obtain

$$(11) \quad \frac{dE(t)}{dt} \exp((\alpha + \theta + \mu_h)t) + (\alpha + \theta + \mu_h) \exp((\alpha + \theta + \mu_h)t) E(t) \geq 0,$$

$$(12) \quad \frac{d}{dt} (\exp((\alpha + \theta + \mu_h)t) E(t)) \geq 0.$$

By integrating this inequality over the interval from 0 to t , we obtain:

$$(13) \quad \int_0^t \frac{d}{ds} (\exp((\alpha + \theta + \mu_h)s) E(s)) ds \geq 0.$$

then

$$(14) \quad E(t) \geq E(0) \exp(-(\alpha + \theta + \mu_h)t),$$

$$(15) \quad E(t) \geq 0.$$

The third equation in system (1) indicates that

$$(16) \quad \begin{aligned} \frac{dI(t)}{dt} &= \alpha E(t) - (\gamma + \mu_h + \sigma) I(t) \\ &\geq -(\gamma + \mu_h + \sigma) I(t). \end{aligned}$$

Then

$$(17) \quad \frac{dI(t)}{dt} + (\gamma + \mu_h + \sigma) I(t) \geq 0.$$

Multiplying both sides of the last inequality by $\exp((\gamma + \mu_h + \sigma)t)$ gives us

$$(18) \quad \frac{dI(t)}{dt} \exp((\gamma + \mu_h + \sigma)t) + (\gamma + \mu_h + \sigma) \exp((\gamma + \mu_h + \sigma)t) I(t) \geq 0,$$

$$(19) \quad \frac{d}{dt} (I(t) \exp((\gamma + \mu_h + \sigma)t)) \geq 0.$$

When this inequality is integrated over the interval from 0 to t , it results in:

$$(20) \quad \int_0^t \frac{d}{ds} (I(s) \exp((\gamma + \mu_h + \sigma)s)) ds \geq 0.$$

Then

$$(21) \quad I(t) \geq I(0) \exp(-(\gamma + \mu_h + \sigma)t),$$

$$(22) \quad I(t) \geq 0.$$

Correspondingly, we demonstrate $V(t) \geq 0$, $R(t) \geq 0$, $I_a(t) \geq 0$ and $R(t) \geq 0$ □

2.1.2. Boundedness of the solutions.

Theorem 2.

The collection

$$(23) \quad \left\{ \begin{array}{l} \Omega_h = \left\{ (S, E, I, V, R) \in \mathbb{R}_+^5 : 0 \leq S + E + I + H + R \leq \frac{\Lambda}{\mu_h} \right\}, \\ \Omega_a = \left\{ (S_a, I_a) \in \mathbb{R}_+^2 : 0 \leq S_a + I_a \leq \frac{\Lambda_1}{\mu_a} \right\}. \end{array} \right.$$

Maintains positive invariance within system (1) given the specified initial conditions

$$S(0) \geq 0, E(0) \geq 0, A(0) \geq 0, I(0) \geq 0, H(0) \geq 0, I_a(0) \geq 0, S_a(0) \geq 0 \text{ and } R(0) \geq 0$$

Proof.

As defined

$$(24) \quad N_h = E + S + V + R + I.$$

Therefore

$$(25) \quad \frac{dN_h}{dt} = \Lambda - \mu_h N_h - \sigma I(t),$$

$$(26) \quad \frac{dN_h}{dt} = \Lambda - \mu_h N_h - \sigma I(t) \leq -\mu_h N_h + \Lambda,$$

$$(27) \quad \frac{dN_h}{dt} \leq -\mu_h N_h + \Lambda,$$

$$(28) \quad N_h(t) \leq \frac{\Lambda}{\mu_h} (1 - e^{-\mu_h t}) + N_h(0) e^{-\mu_h t}.$$

Taking the limit as $t \rightarrow \infty$, we obtain $\limsup_{t \rightarrow \infty} N_h(t) = \frac{\Lambda}{\mu_h}$.

Consequently, the region Ω_h is confirmed to be a positively invariant set for the system (1).

$$(29) \quad N_h(t) \leq \frac{\Lambda}{\mu_h}.$$

Following this, it can be demonstrated that

$$(30) \quad N_a(t) \leq \frac{\Lambda_1}{\mu_a}.$$

□

2.2. Existence and uniqueness of solutions.

Theorem 3.

The system (1), given the initial conditions $(S(0), E(0), I(0), V(0), R(0), I_a(0), S_a(0))$, possesses a unique solution. This ensures that for any set of initial values within the specified range, the behavior of the system can be precisely determined.

Proof.

Thus, system (1) can be reformulated as follows: $\Phi(X(t)) = AX + B(X(t))$

where

$$(31) \quad X = \begin{pmatrix} S \\ E \\ I \\ V \\ R \\ S_a \\ I_a \end{pmatrix}, \quad \Phi(B(X)) = \begin{pmatrix} \frac{dS}{dt} \\ \frac{dE}{dt} \\ \frac{dI}{dt} \\ \frac{dV}{dt} \\ \frac{dR}{dt} \\ \frac{dS_a}{dt} \\ \frac{dI_a}{dt} \end{pmatrix}$$

and

$$A = \begin{pmatrix} -\mu_1 - \lambda & 0 & 0 & 0 & 0 & 0 & 0 \\ 0 & B_1 & 0 & 0 & 0 & 0 & 0 \\ 0 & \alpha & B_2 & 0 & 0 & 0 & 0 \\ \lambda & \theta & \gamma & B_3 & 0 & 0 & 0 \\ 0 & 0 & 0 & n & -\mu_5 & 0 & 0 \\ 0 & 0 & 0 & 0 & 0 & -\mu_6 & 0 \\ 0 & 0 & 0 & 0 & 0 & 0 & -\mu_7 \end{pmatrix}.$$

Where $B_1 = -(\alpha + \theta + \mu_2)$, $B_2 = -(\gamma + \sigma + \mu_3)$ and $B_3 = -(\chi_4 + \mu_4)$.

As well as

$$B(X(t)) = \begin{pmatrix} \Lambda - \beta_1 \frac{I(t)S(t)}{N_h} - \beta_2 \frac{I_a(t)S(t)}{N_h} \\ \beta_1 \frac{I(t)S(t)}{N_h} + \beta_2 \frac{I_a(t)S(t)}{N_h} \\ 0 \\ 0 \\ 0 \\ 0 \\ \Lambda_1 - \beta_3 \frac{S_a(t)I_a(t)}{N_a} \\ \beta_3 \frac{S_a(t)I_a(t)}{N_a} \end{pmatrix}.$$

Given that X_1 and X_2 are solutions of (1), we have

$$\begin{aligned} |B(X_1) - B(X_2)| &\leq 2 \left| \beta_1 \frac{S_1 I_1}{N_h} + \beta_2 \frac{S_1 I_{a1}}{N_h} - \beta_1 \frac{S_2 I_2}{N_h} - \beta_2 \frac{S_2 I_{a2}}{N_h} \right| + 2 \left| \beta_3 \frac{S_{a1} I_{a1}}{N_a} - \beta_3 \frac{S_{a2} I_{a2}}{N_a} \right|, \\ &= 2 \left| \frac{\beta_1 S_1}{N_h} (I_1 - I_2) + \frac{\beta_1 I_2}{N_h} (S_1 - S_2) + \frac{\beta_2 S_1}{N_h} (I_{a1} - I_{a2}) + \frac{\beta_2 I_{a2}}{N_h} (S_1 - S_2) \right| + 2 \left| \frac{\beta_3 S_{a1}}{N_a} (I_{a1} - I_{a2}) + \frac{\beta_3 I_{a2}}{N_a} (S_{a1} - S_{a2}) \right|, \\ &\leq 2 \left(\frac{\beta_1 S_1}{N_h} |I_1 - I_2| + \frac{\beta_1 I_2}{N_h} |S_1 - S_2| + \frac{\beta_2 S_1}{N_h} |I_{a1} - I_{a2}| + \frac{\beta_2 I_{a2}}{N_h} |S_1 - S_2| \right) + 2 \left(\frac{\beta_3 S_{a1}}{N_a} |I_{a1} - I_{a2}| + \frac{\beta_3 I_{a2}}{N_a} |S_{a1} - S_{a2}| \right). \end{aligned}$$

Where

$$(32) \quad |S_1| \leq \frac{\Lambda}{N_h}, \quad |I_2| \leq \frac{\Lambda}{N_h}, \quad |S_{a1}| \leq \frac{\Lambda_1}{N_a} \quad \text{and} \quad |I_{a2}| \leq \frac{\Lambda_1}{N_a},$$

$$(33) \quad |B(X_1) - B(X_2)| \leq \frac{2\Lambda}{N_h} (\beta_1 |I_1 - I_2| + \beta_1 |S_1 - S_2| + \beta_2 |I_{a1} - I_{a2}| + \beta_2 |S_1 - S_2|) + \frac{2\Lambda_1}{N_a} (\beta_3 |I_{a1} - I_{a2}| + \beta_3 |S_{a1} - S_{a2}|).$$

By extracting the common factor, we derive:

$$(34) \quad \begin{aligned} \|\Phi(X_1) - \Phi(X_2)\| &\leq \frac{2\Lambda}{N_h} (\beta_1 + \beta_2) |S_1 - S_2| + \frac{2\beta_1 \Lambda}{N_h} |I_1 - I_2| \\ &\quad + \left(\frac{2\beta_2 \Lambda}{N_h} + \frac{2\beta_3 \Lambda_1}{N_a} \right) |I_{a1} - I_{a2}| + \frac{2\beta_3 \Lambda_1}{N_a} |S_{a1} - S_{a2}|, \\ &\leq N \|X_1 - X_2\|. \end{aligned}$$

where

$$(35) \quad N = \max \left(\frac{2\Lambda}{N_h} (\beta_1 + \beta_2), \frac{2\beta_1 \Lambda}{N_h}, \frac{2\beta_2 \Lambda}{N_h} + \frac{2\beta_3 \Lambda_1}{N_a}, \frac{2\beta_3 \Lambda_1}{N_a}, \|\Lambda\| \right).$$

Therefore, it follows that the function B is uniformly Lipschitz continuous. Moreover, with the constraints $S(t) \geq 0$, $E(t) \geq 0$, $I(t) \geq 0$, $V(t) \geq 0$, $R(t) \geq 0$, $S_a(t) \geq 0$, and $I_a(t) \geq 0$ in \mathbb{R}_+^7 , we conclude that a solution to the system exists. This ensures that the non-negativity conditions for the variables are maintained, thereby validating the existence of a solution under the given initial conditions and system constraints [25]. \square

3. THE CONTROLLED MATHEMATICAL MODEL

Our control strategies aim to elevate public awareness and caution regarding the disease. This is achieved through educational and outreach campaigns designed to enhance public knowledge. The primary objective is to safeguard individuals by promoting awareness, encouraging the infected to seek medical care in hospitals, advocating for vaccination, and avoiding direct contact with infected individuals or animals. These efforts concentrate on increasing vigilance through advocacy campaigns and calls for alertness to prevent the disease while minimizing the costs associated with implementing the control strategy.

The model system (1) is refined by introducing two control variables, $u(t)$ and $v(t)$, within the time interval $t \in [0, t_f]$.

$$(36) \quad \left\{ \begin{array}{l} \frac{dS(t)}{dt} = \Lambda - \beta_1 \frac{S(t)I(t)}{N} (1 - u(t)) - \beta_2 \frac{S(t)I_a(t)}{N} (1 - v(t)) - (\lambda + \mu_h)S(t), \\ \frac{dE(t)}{dt} = \beta_1 \frac{S(t)I(t)}{N} (1 - u(t)) + \beta_2 \frac{S(t)I_a(t)}{N} (1 - v(t)) - (\alpha + \theta + \mu_h)E(t), \\ \frac{dI(t)}{dt} = \alpha E(t) - (\gamma + \mu_h + \sigma)I(t), \\ \frac{dV(t)}{dt} = \gamma I(t) + \lambda S(t) + \theta E(t) - (n + \mu_h)V(t), \\ \frac{dR(t)}{dt} = nV(t) - \mu_h R(t), \\ \frac{dS_a(t)}{dt} = \Lambda_1 - \beta_3 \frac{S_a(t)I_a(t)}{N} - \mu_a S_a(t), \\ \frac{dI_a(t)}{dt} = \beta_3 \frac{S_a(t)I_a(t)}{N} - \mu_a I_a(t). \end{array} \right.$$

where $(S(0), E(0), I(0), V(0), R(0), S_a(0), I_a(0)) \in \mathbb{R}_+^7$ represent the specified initial state.

The control variable v represents the vaccination administered to individuals infected with the disease. The control variable w signifies efforts to reduce the gatherings of non-infected individuals with those infected or with disease-carrying animals through awareness campaigns and the implementation of vector control measures.

4. THE OPTIMAL CONTROL PROBLEM

The challenge lies in minimizing the objective functional, aiming to achieve an optimal balance between the control measures and their associated costs.

(37)

$$J(u, v) = I(T) + I_a(T) + E(T) - R(T) + \int_0^t \left(I(t) + I_a(t) + E(t) - R(t) + \frac{a_1}{2} u^2(t) + \frac{a_2}{2} v^2(t) \right) dt.$$

The coefficients $a_1 \geq 0$ and $a_2 \geq 0$ represent the cost factors, chosen to balance the relative importance of $u(t)$ and $v(t)$ at time t , and $t_f = T$ represents the concluding time.

In essence, we aim to find the optimal controls u^* and v^* such that

$$(38) \quad J(u^*, v^*) = \min_{(u,v) \in V_{ad}} J(u, v).$$

where V denotes the set of permissible controls, which is defined by the following constraints:

(39)

$$V_{ad} = \{(u, v) / 0 \leq u_{\min} \leq u(t) \leq u_{\max} \leq 1 \quad \text{and} \quad 0 \leq v_{\min} \leq v(t) \leq v_{\max} \leq 1 \quad \text{for } t \in [0, t_f]\}.$$

4.1. The presence of an optimal control.

Theorem 4.

Consider the task of regulating system (36). There exists an optimal control $(u^(t), v^*(t)) \in V_{ad}$ such that*

$$(40) \quad J(u^*(t), v^*(t)) = \min_{(u,v) \in V_{ad}} J(u(t), v(t)).$$

provided that the following conditions are met:

- 1. The set of control actions V_{ad} and the corresponding state variables are nonempty.*
- 2. The right-hand side of the system is bounded by a linear function of the state and control variables.*
- 3. The control set V_{ad} is convex and closed.*
- 4. The integral $N(S, E, I, V, R, S_a, I_a, u, v)$ in the objective function is convex over the set of admissible controls V_{ad} .*

Proof.

Condition 1.

To demonstrate that the set of control actions and the associated state variables is non-empty, we utilize a simplified existence result from Boyce and DiPrima in [26].

Consider the system described by $\dot{Y}_i = Y_{K_i}(t, Y_1, Y_2, Y_3, Y_4, Y_5, Y_6, Y_7)$ for $i \in \{1, \dots, 7\}$, where $(Y_1, Y_2, Y_3, Y_4, Y_5, Y_6, Y_7) = (S, E, I, V, R, S_a, I_a)$. The functions $Y_S, Y_E, Y_I, Y_V, Y_R, Y_{S_a}, Y_{I_a}$ and Z_R represent the right-hand side of equation (4). Let the control functions be defined as $u(t) = c_1$ and $v(t) = c_2$ for some constants c_1, c_2 . Given that all parameters are constants and $K_1, K_2, K_3, K_4, K_5, K_6$ and K_7 are continuous functions, it follows that $Y_S, Y_E, Y_I, Y_V, Y_R, Y_{S_a}$ and Y_{I_a} are also continuous. Additionally, the partial derivatives $\frac{\partial Y_{K_i}}{\partial K_i}$ for $i \in \{1, \dots, 7\}$ are continuous.

Therefore, there exists a unique solution $(S, E, I, V, R, S_a, I_a)$ satisfying the initial conditions. Consequently, the set of control actions and their corresponding state variables is non-empty, thereby satisfying the first condition.

Condition 2.

By definition, the set of admissible controls V_{ad} is closed. Consider any controls $(u, v) \in V_{ad}$ and $\tau \in [0, 1]$. We need to show that $0 \leq \tau u + (1 - \tau)v \leq 1$. Indeed, we observe that $\tau u \leq \tau$ and $(1 - \tau)v \leq (1 - \tau)$, which implies that $\tau u + (1 - \tau)v \leq \tau + (1 - \tau) = 1$. Therefore, we have $0 \leq \tau v + (1 - \tau)v \leq 1$ for all $(u, v) \in V_{ad}$ and $\tau \in [0, 1]$. This demonstrates that V_{ad} is both closed and convex, thereby satisfying the second condition.

Condition 3.

The right-hand sides of the equations in system (36) are continuous and are limited by the combination of the bounded state variables and control inputs. Moreover, they can be described as a linear function of u and v , with coefficients that vary with both the state variables and time.

Condition 4.

The integral within the objective function $I(t) + I_a(t) + E(t) - R(t) + \frac{a_1}{2}u^2(t) + \frac{a_2}{2}v^2(t)$ is inherently convex over the set V_{ad} . Indeed, there exist constants Φ_1 and Φ_2 , with $\beta > 1$, such that the integral in the objective functional satisfies:

$$(41) \quad N(S, E, I, V, R, S_a, I_a, u, v) \geq \Phi_1 + \Phi_2(|u|^2 + |v|^2)^{\frac{\kappa}{2}},$$

where

$$(42) \quad I(t) + I_a(t) + E(t) - R(t) + \frac{a_1}{2}u^2(t) + \frac{a_2}{2}v^2(t) \geq \Phi_1 + \Phi_2(|u|^2 + |v|^2)^{\frac{\kappa}{2}}.$$

Given that the state variables are bounded, let:

$$(43) \quad \Phi_1 = 4 \inf_{t \in [0, T]} (I(t) + I_a(t)) + E(t) - R(t), \quad \Phi_2 = \inf \left(\frac{a_1}{2}, \frac{a_2}{2} \right), \quad \text{and} \quad \kappa = 2.$$

Therefore, based on the results presented by Fleming and Richel in [27] and see [28], we can assert the existence of an optimal control. \square

4.2. Defining optimal control characterization.

In this section, we apply Pontryagin's maximum principle [29, 30, 31, 32, 33]. The core idea is to introduce the adjoint function, which establishes a link between the differential equation system and the objective functional. This linkage results in the creation of a function known as the Hamiltonian.

Pontryagin's principle shifts the challenge of finding an optimal control for the objective functional, given initial conditions, to the problem of finding a control that optimizes the Hamiltonian at each point in time.

We now define the Hamiltonian H at time t as follows:

$$(44) \quad H = I(t) + I_a(t) + E(t) - R(t) + \frac{a_1}{2}u^2(t) + \frac{a_2}{2}v^2(t) + \sum_{i=1}^7 \chi_i(t) \cdot q_i$$

In this context, q_i represents the right-hand side of the differential equations system (36) for the i -th state variable, and χ_i are the corresponding adjoint functions. These adjoint functions are associated with the state variables and are utilized to reflect the influence of state changes on the cost functional.

Theorem 5.

Assume that $(u^, v^*) \in V_{ad}$ represents the optimal control variables, and let $S^*, E^*, I^*, H^*, V^*, S_a^*$ and I_a^* be the corresponding optimal trajectories for the state variables. There are adjoint functions $\chi_1, \chi_2, \chi_3, \chi_4, \chi_5, \chi_6$ and χ_7 that satisfy the following conditions:*

$$(45) \quad \begin{aligned} \chi_1' &= -\frac{\partial H}{\partial S} = \beta_1 \frac{I}{N} (1 - u(t)) (\chi_1 - \chi_2) + \beta_2 \frac{I_a}{N} (1 - v(t)) (\chi_1 + \chi_7 - \chi_2) - \chi_4 \lambda + \chi_1 (\lambda + \mu_h), \\ \chi_2' &= -\frac{\partial H}{\partial E} = -1 + \theta (\chi_2 + \chi_4) + \alpha (\chi_2 - \chi_3) - \xi_2 \mu_h, \\ \chi_3' &= -\frac{\partial H}{\partial I} = -1 + \beta_1 \frac{S}{N} (1 - u(t)) (\chi_1 - \chi_2) + \gamma (\chi_3 - \chi_4) + \chi_3 (\sigma + \mu_h), \\ \chi_4' &= -\frac{\partial H}{\partial V} = n (\chi_4 - \chi_5) - \chi_4 \mu_h, \end{aligned}$$

$$\begin{aligned}\chi_5' &= -\frac{\partial H}{\partial R} = 1 + \chi_5 \mu_h, \\ \chi_6' &= -\frac{\partial H}{\partial S_a} = \beta_3 \frac{I_a}{N} (\chi_6 - \chi_7) + \chi_6 \mu_a, \\ \chi_7' &= -\frac{\partial H}{\partial I_a} = -1 + \beta_3 \frac{S_a}{N} (\chi_6 - \chi_7) + \chi_7 \mu_a.\end{aligned}$$

Under the transversality conditions

$$\begin{aligned}\chi_1(t_f) &= 0, \quad \chi_2(t_f) = 1, \quad \chi_3(t_f) = 1, \quad \chi_4(t_f) = 0, \\ \chi_5(t_f) &= -1, \quad \chi_6(t_f) = 0, \quad \chi_7(t_f) = 1.\end{aligned}$$

The solution to the optimal control problem is provided by the control variables u^* and v^* . The optimal control values are determined as follows:

$$(46) \quad \begin{aligned}u^* &= \min \left(1, \max \left(0, \frac{(\chi_2(t) - \chi_1(t)) \beta_1 S(t) I(t)}{a_1 N_h} \right) \right), \\ v^* &= \min \left(1, \max \left(0, \frac{(\chi_2(t) - \chi_1(t)) \beta_2 S(t) I_a(t)}{a_2 N_h} \right) \right).\end{aligned}$$

Proof.

The Hamiltonian H at a given time t can be expressed as follows:

$$(47) \quad \begin{aligned}H &= I(T) + I_a(T) + E(T) - R(T) + \frac{a_1}{2} u^2(t) + \frac{a_2}{2} v^2(t) \\ &+ \chi_1 \left\{ \Lambda - \beta_1 \frac{S(t)I(t)}{N} (1 - u(t)) - \beta_2 \frac{S(t)I_a(t)}{N} (1 - v(t)) - (\lambda + \mu_h) S(t) \right\} \\ &+ \chi_2 \left\{ \beta_1 \frac{S(t)I(t)}{N} (1 - u(t)) + \beta_2 \frac{S(t)I_a(t)}{N} (1 - v(t)) - (\alpha + \theta + \mu_h) E(t) \right\} \\ &+ \chi_3 \{ \alpha E(t) - (\gamma + \mu_h + \sigma) I(t) \} \\ &+ \chi_4 \{ \gamma I(t) + n S(t) + \theta E(t) - (n + \mu_h) V(t) \} + \chi_5 \{ \chi V(t) - \mu_h R(t) \} \\ &+ \chi_6 \left\{ \Lambda_1 - \beta_3 \frac{S_a(t)I_a(t)}{N} - \mu_a S_a(t) \right\} \\ &+ \chi_7 \left\{ \beta_3 \frac{S_a(t)I_a(t)}{N} - \mu_a I_a(t) \right\}.\end{aligned}$$

Utilizing Pontryagin's maximum principle [23], we derived the adjoint equations and the transversality conditions, which are represented as follows:

$$\chi_1' = -\frac{\partial H}{\partial Y_i} \text{ and } \chi_i(t_f) = 0 \text{ for } i \in \{1, 4, 6\},$$

where $(Y_1, Y_2, Y_3, Y_4, Y_5, Y_6, Y_7) = (S, E, I, V, R, S_a, I_a)$

The transversality conditions imply that at the terminal time, the adjoint variables must be perpendicular to the feasible set of the terminal state. This condition ensures the proper formulation

of the optimal control problem, thereby providing a stable solution. The optimality conditions will be applied to derive the optimal controls $u^*(t)$ and $v^*(t)$ for $t \in [0, t_f]$.

$$(48) \quad \frac{\partial H}{\partial u} = 0 \quad \text{and} \quad \frac{\partial H}{\partial v} = 0$$

subsequently,

$$(49) \quad \begin{aligned} \frac{\partial H}{\partial u} &= a_1 u + \chi_1 \left(\beta_1 \frac{S(t)I(t)}{N_h} \right) - \chi_2 \left(\beta_1 \frac{S(t)I(t)}{N_h} \right) = 0, \\ \frac{\partial H}{\partial v} &= a_2 v + \chi_1 \left(\beta_2 \frac{S(t)I_a(t)}{N_h} \right) - \chi_2 \left(\beta_2 \frac{S(t)I_a(t)}{N_h} \right) = 0. \end{aligned}$$

Therefore,

$$(50) \quad \begin{aligned} u^* &= \frac{(\chi_2(t) - \chi_1(t)) \beta_1 \frac{S(t)I(t)}{N_h}}{a_1}, \\ v^* &= \frac{(\chi_2(t) - \chi_1(t)) \beta_2 \frac{S(t)I_a(t)}{N_h}}{a_2}. \end{aligned}$$

As a result of the constraints within V_{ad} for the control variables, we can efficiently determine the optimal controls $u^*(t)$ and $v^*(t)$ as expressed in equations (46). \square

5. SIMULATION

In this section, we analyze the outcomes from the numerical solution of the optimality system. In the formulated control problem, initial conditions are applied to the state variables, while terminal conditions are imposed on the adjoint variables. The optimality system forms a two-point boundary value problem with specific boundary conditions at $t = 0$ and $t = T$. This system is solved iteratively, starting with a forward computation of the state equations, followed by a backward computation of the adjoint equations. An initial guess for the control variables is provided in the first iteration. Before each subsequent iteration, the control variables are updated according to their defined characteristics. This iterative process continues until convergence between successive iterations is reached. The code for solving the optimality system was written and executed in MATLAB.

Figure (4) shows the development of individuals exposed to viral infection. We notice a gradual increase in the number of individuals exposed to the virus, and over time this rapid increase indicates that the symptoms of infection begin to appear more clearly, leading to the emergence of a group in which the infection is evident Figure (5). The number of virus carriers remains

high over time, which significantly contributes to the spread of the virus among people. This transformation occurs due to interactions between susceptible individuals and bats or pigs that carry the virus.

In this article, we utilized the parameter values presented in Table (2). These values were chosen based on hypothetical scenarios due to the unavailability of real-world data. This decision was made to ensure that our model could still be constructed and analyzed effectively in the absence of empirical data. By relying on hypothetical data, we aimed to explore a wide range of possible outcomes and dynamics within the model. This approach also allows for a comprehensive analysis of the model's behavior under various conditions, which can later be validated against real-world data once it becomes available. Additionally, using hypothetical scenarios helps identify potential limitations and areas for further research, ensuring that our model remains robust and adaptable to different contexts.

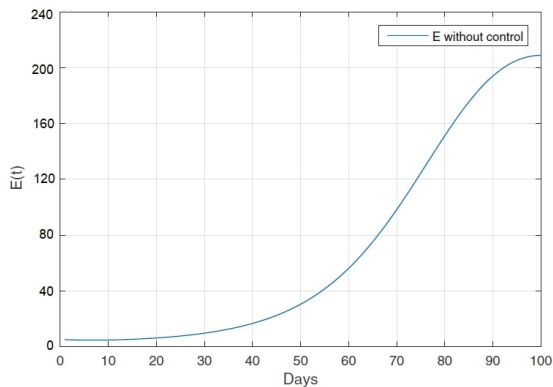


FIGURE 4. The evolution of Exposed (E) without control.

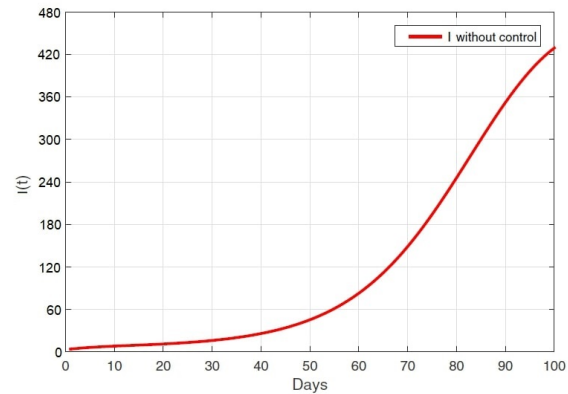


FIGURE 5. The evolution of Infected (I) without control.

The parameter values for the model were determined using hypothetical scenarios, as real-world data was unavailable. This approach was necessary due to the lack of actual data to inform our selections. The corresponding data can be found in Table (2).

Parameter	Description	value in d^{-1}
Λ	The rate of new births among the human population.	350
Λ_1	The rate of new births among the animals population.	0.5
β_1	The rate at which the virus is transmitted between an infected individual and a susceptible person.	0.22
β_2	The transmission rate of the virus between an infected animal and a susceptible human.	0.18
β_3	The rate at which the virus is transmitted from an infected animal to a susceptible animal.	0.25
α	Percentage of asymptomatic infected individuals.	0.35
γ	Percentage of infected individuals.	0.002
\mathbf{n}	The rate at which individuals recover.	0.35
σ	Mortality rate due to viral infection.	0.002
μ	Intrinsic mortality rate.	0.0002
λ	Percentage of susceptible person.	0.3

TABLE 2. Description of the parameters of the nipah model.

DISCUSSION

In this section, we focus on the numerical evaluation of various optimal control strategies for managing the Nipah virus, a highly infectious disease with significant mortality rates. Our strategies include awareness initiatives through media and educational programs highlighting the severity of the Nipah virus, safety campaigns to avoid direct contact with infected individuals, and promoting the uptake of necessary vaccinations and medical care. Numerical simulations are crucial for assessing the effectiveness of these strategies.

By implementing these control measures in our mathematical model, we can observe their impact on disease dynamics. For instance, awareness campaigns can significantly reduce infection rates by increasing public knowledge and encouraging preventive behaviors, as shown in similar studies on infectious diseases like measles and Ebola. Avoiding direct contact through safety campaigns and promoting vaccinations and medical care can further mitigate the spread of the Nipah virus and improve public health outcomes.

The numerical solutions for the Nipah virus control strategies were computed using MATLAB,

leveraging specific parameter values and initial state variable values. This approach allows for a thorough examination of different strategies and their potential to control the disease effectively. Recent research on the optimal control of infectious diseases emphasizes the importance of integrating multiple strategies to achieve the best outcomes. For example, studies on the control of the Ebola virus demonstrated that combining quarantine measures, public awareness, and vaccination efforts can significantly reduce the spread of the disease.

5.1. Strategy 1: Protect susceptible people from contact with infected people using control u .

We only used the optimal control $u(t)$. This strategy aims to reduce the number of infected people and increase the number of those protected against the virus. By applying various strategies, such as educating people about the dangers of infection with this virus through awareness programs and direct and indirect awareness-raising meetings using social media platforms, it became clear that this strategy led to positive results Figures (6,7).

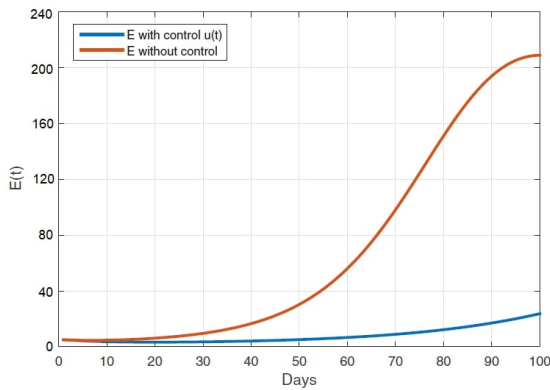


FIGURE 6. The compartment E with control u .

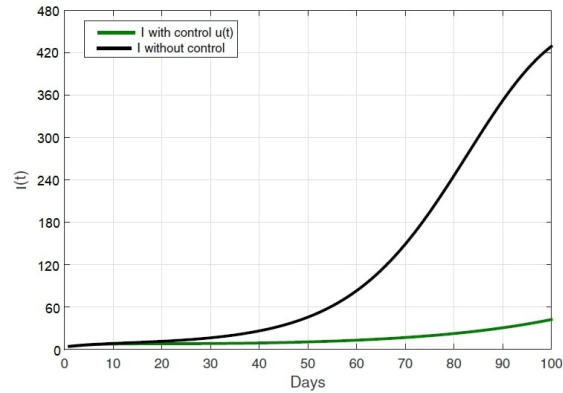


FIGURE 7. The compartment I with control u .

5.2. Strategy 2: Vaccinate infected and uninfected people and adopt quarantine in affected areas using control v .

A quarantine strategy was adopted for infected and vaccinated individuals, in addition to restricting entry and exit from neighborhoods and areas known for spreading the virus. This measure led to a decrease in the number of exposed (8) and infected (9) individuals with the Nipah virus, and an increase in the number of recovered individuals (10).

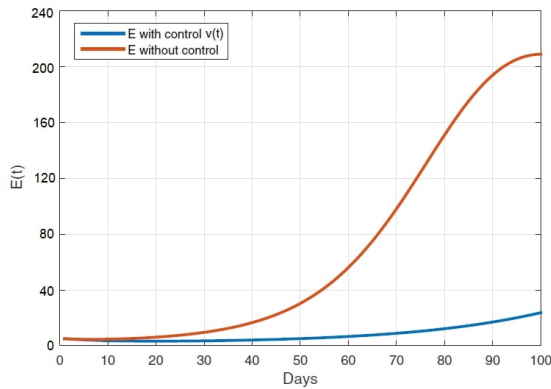


FIGURE 8. The compartment E with control v .

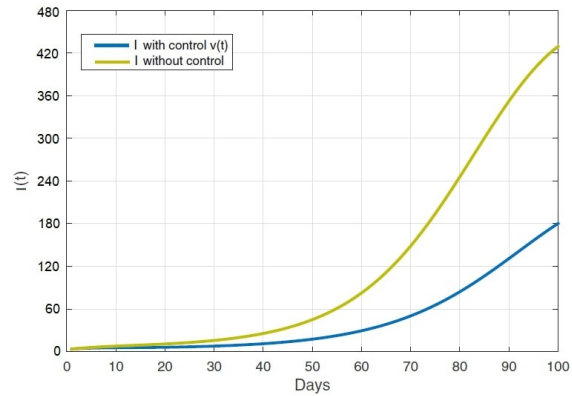


FIGURE 9. The compartment I with control v .

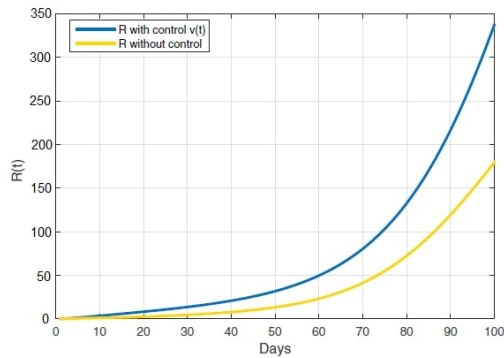


FIGURE 10. The compartment R with control v .

5.3. Strategy 3: Encourage exposed people to join quarantine centers and avoid contact with infected people and infected animals using u and v .

In this strategy, a set of preventive measures were adopted, such as raising awareness and conducting a series of awareness campaigns among all citizens to inform them of the dangers of the virus through the media. All preventive measures were taken to avoid infection. These measures include wearing masks, washing hands regularly, and avoiding contact with infected bats or pigs. If some side effects appear, one should go to the hospital immediately and as quickly as possible, which will help limit the spread of the virus as shown in the figures (11) and (12).

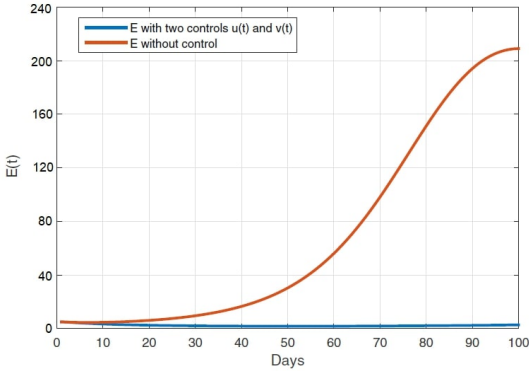


FIGURE 11. The compartment E with control u and v.

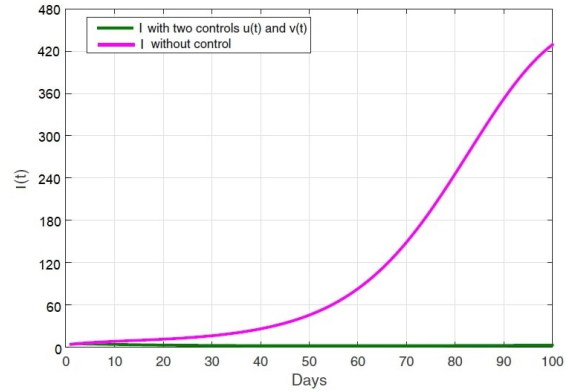


FIGURE 12. The compartment I with control u and v.

6. CONCLUSION

In this study, we introduce a novel model aimed at achieving a more accurate and detailed understanding of the dynamics of Nipah virus (NiV) transmission among individuals. Our model transcends theoretical boundaries, becoming a practical tool capable of transforming infectious disease management. By incorporating robust control strategies, the model aims to reduce the number of infections. We compare scenarios with and without the application of control measures, demonstrating that implementing control significantly reduces infection rates. To provide a comprehensive view of NiV transmission, we include detailed graphs showing the numbers of infected and exposed individuals under both controlled and uncontrolled conditions.

Our findings confirm the effectiveness of control measures in curbing the spread of NiV and enhancing recovery rates. Integrating this model into public health strategies represents significant progress in the global fight against infectious diseases. Promoting vaccine use, encouraging infected individuals to seek medical treatment through awareness campaigns, and emphasizing the importance of avoiding close contact with bats, pigs, and infected persons are key strategies to reduce disease transmission.

Looking ahead, we aim to explore the use of fractional derivatives within a spatiotemporal framework to deepen our understanding of NiV transmission dynamics. This approach promises to capture complex spatial and temporal patterns, thereby enhancing the accuracy of disease forecasts and control strategies.

CONFLICT OF INTERESTS

The authors declare that there is no conflict of interests.

REFERENCES

- [1] S. Srivastava, P.K. Sharma, S. Gurjar, et al. Nipah Virus Strikes Kerala: Recent Cases and Implications, *The Egyptian Journal of Internal Medicine* 36 (2024), 11. <https://doi.org/10.1186/s43162-024-00276-x>.
- [2] M.Y. Khan, S. Ullah, M. Farooq, et al. Optimal Control Analysis for the Nipah Infection with Constant and Time-Varying Vaccination and Treatment under Real Data Application, *Sci. Rep.* 14 (2024), 17532. <https://doi.org/10.1038/s41598-024-68091-6>.
- [3] A.C. Loyinmi, S.O. Gbodogbe, Mathematical Modeling and Control Strategies for Nipah Virus Transmission Incorporating Bat-To-Pig-To-Human Pathway, *EDUCATUM J. Sci. Math. Technol.* 11 (2024), 54–80. <https://doi.org/10.37134/ejsmt.vol11.1.7.2024>.
- [4] K.B. Chua, W.J. Bellini, P.A. Rota, et al. Nipah Virus: A Recently Emergent Deadly Paramyxovirus, *Science* 288 (2000), 1432–1435. <https://doi.org/10.1126/science.288.5470.1432>.
- [5] K.B. Chua, Nipah Virus Outbreak in Malaysia, *J. Clin. Virol.* 26 (2003), 265–275. [https://doi.org/10.1016/S1386-6532\(02\)00268-8](https://doi.org/10.1016/S1386-6532(02)00268-8).
- [6] J. Faus-Cotino, G. Reina, J. Pueyo, Nipah Virus: A Multidimensional Update, *Viruses* 16 (2024), 179. <https://doi.org/10.3390/v16020179>.
- [7] P.N. Bashetti, C. Avhad, A. Kshirsagar, et al. Navigating Nipah Virus Outbreaks: Epidemiology, One Health Strategies, and Pathological Insights in India, *Int. J. Vet. Sci. Anim. Husb.* 9 (2024), 1441–1446.
- [8] H. Barnes, The Theory of Realistic Mathematics Education as a Theoretical Framework for Teaching Low Attainers in Mathematics, *Pythagoras* 61 (2005), 42–57. <https://doi.org/10.4102/pythagoras.v0i61.120>.
- [9] B. Thomas, P. Chandran, M. Lilabi, et al. Nipah Virus Infection in Kozhikode, Kerala, South India, in 2018: Epidemiology of an Outbreak of an Emerging Disease, *Indian J. Community Med.* 44 (2019), 383–387. https://doi.org/10.4103/ijcm.IJCM_198_19.
- [10] P.D. Yadav, R.R. Sahay, A. Balakrishnan, et al. Nipah Virus Outbreak in Kerala State, India Amidst of COVID-19 Pandemic, *Front. Public Health* 10 (2022), 818545. <https://doi.org/10.3389/fpubh.2022.818545>.
- [11] M.D. Gabra, H.S. Ghaith, M.A. Ebada, Nipah Virus: An Updated Review and Emerging Challenges, *Infect. Disord. - Drug Targets* 22 (2022), e170122200296. <https://doi.org/10.2174/1871526522666220117120859>.
- [12] F. Evirgen, Transmission of Nipah Virus Dynamics under Caputo Fractional Derivative, *J. Comput. Appl. Math.* 418 (2023), 114654. <https://doi.org/10.1016/j.cam.2022.114654>.

- [13] L. Bruno, M.A. Nappo, L. Ferrari, et al. Nipah Virus Disease: Epidemiological, Clinical, Diagnostic and Legislative Aspects of This Unpredictable Emerging Zoonosis, *Animals* 13 (2022), 159. <https://doi.org/10.3390/ani13010159>.
- [14] S.P. Luby, E.S. Gurley, M.J. Hossain, Transmission of Human Infection with Nipah Virus, *Clin. Infect. Dis.* 49 (2009), 1743–1748. <https://doi.org/10.1086/647951>.
- [15] J.M. Yob, H. Field, A.M. Rashdi, et al. Nipah Virus Infection in Bats (Order Chiroptera) in Peninsular Malaysia, *Emerg. Infect. Dis.* 7 (2001), 439–441. <https://doi.org/10.3201/eid0703.010312>.
- [16] U.D. Parashar, L.M. Sunn, F. Ong, et al. Case-Control Study of Risk Factors for Human Infection with a New Zoonotic Paramyxovirus, Nipah Virus, during a 1998–1999 Outbreak of Severe Encephalitis in Malaysia, *J. Infect. Dis.* 181 (2000), 1755–1759. <https://doi.org/10.1086/315457>.
- [17] K.S. Tan, C.T. Tan, K.J. Goh, Epidemiological Aspects of Nipah Virus Infection, *Neurol. J. Southeast Asia* 4 (1999), 77–81.
- [18] A.W. Mounts, H. Kaur, U.D. Parashar, et al. A Cohort Study of Health Care Workers to Assess Nosocomial Transmissibility of Nipah Virus, Malaysia, 1999, *J. Infect. Dis.* 183 (2001), 810–813. <https://doi.org/10.1086/318822>.
- [19] J. Sultana, C. N. Podder, Mathematical Analysis of Nipah Virus Infections Using Optimal Control Theory, *J. Appl. Math. Phys.* 04 (2016), 1099–1111. <https://doi.org/10.4236/jamp.2016.46114>.
- [20] M.K. Mondal, M. Hanif, M.H.A. Biswas, A Mathematical Analysis for Controlling the Spread of Nipah Virus Infection, *Int. J. Model. Simul.* 37 (2017), 185–197. <https://doi.org/10.1080/02286203.2017.1320820>.
- [21] P. Chatterjee, P. Nair, M. Chersich, et al. One Health, “Disease X” & the Challenge of “Unknown” Unknowns, *Indian J. Med. Res.* 153 (2021), 264–271. https://doi.org/10.4103/ijmr.IJMR_601_21.
- [22] A.D. Zewdie, S. Gakkhar, A Mathematical Model for Nipah Virus Infection, *J. Appl. Math.* 2020 (2020), 6050834. <https://doi.org/10.1155/2020/6050834>.
- [23] S. Das, P. Das, P. Das, Control of Nipah Virus Outbreak in Commercial Pig-Farm with Biosecurity and Culling, *Math. Model. Nat. Phenom.* 15 (2020), 64. <https://doi.org/10.1051/mmnp/2020047>.
- [24] Samreen, S. Ullah, R. Nawaz, et al. A Mathematical Study Unfolding the Transmission and Control of Deadly Nipah Virus Infection under Optimized Preventive Measures: New Insights Using Fractional Calculus, *Results Phys.* 51 (2023), 106629. <https://doi.org/10.1016/j.rinp.2023.106629>.
- [25] C.T.H. Baker, G. Monegato, G. vanden Berghe, *Ordinary Differential Equations and Integral Equations*, Elsevier, 2001.
- [26] W.E. Boyce, R.C. DiPrima, D.B. Meade, *Elementary Differential Equations*, Wiley, 2017.
- [27] W.H. Fleming, R. Rishel, *Deterministic and Stochastic Optimal Control*, Springer, New York, 2012. <https://doi.org/10.1007/978-1-4612-6380-7>.

- [28] S. Olaniyi, O.A. Ajala, S.F. Abimbade, Optimal Control Analysis of a Mathematical Model for Recurrent Malaria Dynamics, *Oper. Res. Forum* 4 (2023), 14. <https://doi.org/10.1007/s43069-023-00197-5>.
- [29] L.S. Pontryagin, *Mathematical Theory of Optimal Processes*, Routledge, 2018.
- [30] H. Gourram, M. Baroudi, A. Labzai, M. Belam, Mathematical Modeling and Optimal Control Strategy for the Influenza (H5N1), *Commun. Math. Biol. Neurosci.* 2023 (2023), 113. <https://doi.org/10.28919/cmbn/8199>.
- [31] M. Baroudi, I. Smouni, H. Gourram, et al. Optimizing Control Strategies for Monkeypox through Mathematical Modeling, *Partial Differ. Equ. Appl. Math.* 12 (2024), 100996. <https://doi.org/10.1016/j.padiff.2024.100996>.
- [32] I. Smouni, M. Baroudi, M. Alia, et al. Spatiotemporal Stability Analysis of Soil-Borne Disease Dynamics in Tomato Plants, *Model. Earth Syst. Environ.* 11 (2025), 105. <https://doi.org/10.1007/s40808-024-02187-w>.
- [33] M. Baroudi, H. Gourram, A. Labzai, et al. Mathematical Modeling and Monkeypox's Optimal Control Strategy, *Commun. Math. Biol. Neurosci.* 2023 (2023), 110. <https://doi.org/10.28919/cmbn/8198>.